Received: 21 May 2020 | Revised: 31 July 2020 | Accepted: 8 September 2020

DOI: 10.1002/kin.21435

ARTICLE

WILEY

Homogeneous conversion of NO_x and NH_3 with CH_4, CO, and C_2H_4 at the diluted conditions of exhaust-gases of lean operated natural gas engines

Steffen Schmitt[1] | **Sabrina Schwarz**[2] | **Lena Ruwe**[1,3] | **Jacqueline Horstmann**[1] | **Franziska Sabath**[1] | **Lubow Maier**[4] | **Olaf Deutschmann**[2,4] | **Katharina Kohse-Höinghaus**[1]

[1] Department of Chemistry, Bielefeld University, Bielefeld 33615, Germany

[2] Institute for Chemical Technology and Polymer Chemistry, Karlsruhe Institute of Technology (KIT), Karlsruhe 76131, Germany

[3] Physikalisch-Technische Bundesanstalt (PTB), Braunschweig 38116, Germany

[4] Institute for Catalysis Research and Technology (IKFT), Karlsruhe Institute of Technology (KIT), Eggenstein-Leopoldshafen 76344, Germany

Correspondence
Steffen Schmitt, Department of Chemistry, Bielefeld University, Universitätsstraße 25, Bielefeld, 33615, Germany.
Email: s.schmitt@uni-bielefeld.de
Olaf Deutschmann, Institute for Chemical Technology and Polymer Chemistry, Karlsruhe Institute of Technology (KIT), Engesserstraße 20, Karlsruhe, 76131, Germany.
Email: deutschmann@kit.edu

Steffen Schmitt and Sabrina Schwarz contributed equally to this work.

Funding information
Deutsche Forschungsgemeinschaft, Grant/Award Numbers: KO 1363/34-1, DE659/12-1

Abstract

Understanding gas-phase reactions in model gas mixtures approximating pre-turbine heavy-duty natural gas engine exhaust compositions containing NO, NH_3, NO_2, CH_4, CO, and C_2H_4 is extremely relevant for aftertreatment procedure and catalyst design and is thus addressed in this work. In a plug-flow reactor at atmospheric pressure, five different model gas mixtures were investigated in the temperature range of 700-1 200 K, using species analysis with electron ionization molecular-beam mass spectrometry. The mixtures were designed to reveal influences of individual components by adding NO_2, CH_4, CO, and C_2H_4 sequentially to a highly argon-diluted NO/NH_3 base mixture. Effects of all components on the reactivity for NO_x conversion were investigated both experimentally as well as by comparison with three selected kinetic models. Main results show a significantly increased reactivity upon NO_2 and hydrocarbon addition with lowered NO conversion temperatures by up to 200 K. Methane was seen to be of dominant influence in the carbon-containing mixtures regarding interactions between the carbon and nitrogen chemistry as well as formaldehyde formation. The three tested mechanisms were capable to overall represent the reaction behavior satisfactorily. On this basis, it can be stated that significant gas-phase reactivity was observed among typical constituents of pre-turbine natural gas engine exhaust at moderate temperature.

KEYWORDS
ammonia, exhaust gas aftertreatment, gas-phase kinetics, natural gas engines, nitric oxide

1 | INTRODUCTION

Today, internal combustion engines operated with liquid fuels are already highly optimized; hence, a significant further reduction of fuel consumption is technologically challenging. Therefore, gaseous fuels such as methane and hydrogen seem to become attractive alternatives. Methane, the major component of natural gas, exhibits the highest hydrogen-to-carbon ratio of all hydrocarbons (HCs) and therefore a superior energy-carbon balance. In addition, natural gas engines emit comparably low levels of toxic CO and only moderate amounts of NO_x.[1] These rather low emissions of the greenhouse gas CO_2 and of local pollutants make natural gas engines a promising technology for a wide range of applications. Up to now, they are widely used in stationary applications, that is, in combined heat and power plants for energy production, and in some countries also for transportation vehicles, ships, and even passenger cars. The long-term trend toward natural gas-operated combustion engines, often being interfered by legislative decisions, is supported by an existing natural gas infrastructure in many countries. Although fossil sources currently represent the main feedstock for natural gas, promising alternative concepts like biomethane and power-to-gas technologies can open up further sustainable accesses to the highly valuable energy source methane. In addition, such carbon-neutral approaches have the ability to substantially improve the cradle-to-grave analysis of methane as climate-friendly fuel.

Small natural gas engines are commonly operated under stoichiometric conditions and use the well-established three-way catalyst as exhaust gas aftertreatment to control the emissions of CO, HCs, and NO_x. Operation at lean conditions would however further improve the engine efficiency leading to a greenhouse gas advantage of up to 35% compared with a diesel engine.

A very crucial issue with lean-operated natural gas engines is the release of unburnt HCs, mainly the major fuel component CH_4 with up to over 3 000 ppm. In addition, other small alkanes occurring in natural gas as well as combustion intermediates such as small olefins and formaldehyde (CH_2O), a carcinogenic substance, need to be taken care of. All these HCs can be converted by suitable oxidation catalysts with noble metals as active substances. Even though NO_x emissions are at least slightly lower in comparison with diesel engines,[2] the tightening environmental legislation will make a dedicated NO_x abatement system imperative. The reduction of NO_x emissions from gas engines is commonly achieved by the well-established technology of selective catalytic reduction (SCR), using NH_3 as reducing agent, which is provided by thermolysis and hydrolysis of a urea-water solution known as AdBlue and DEF (Diesel Exhaust Fluid). The injection of this urea-water solution into the tail pipe requests a minimum exhaust gas temperature of approximately 570 K (200°C) to avoid formation of deposits.[3] A much more severe challenge however is the oxidation of methane in the exhaust system because even the best catalysts still require temperatures above 700 K at lean conditions.[4,5]

Consequently, both the SCR and the oxidation catalysts are positioned closer to the engine, so-called "close-coupled catalysts" in contrast to the conventional "underfloor catalysts." The catalytic converters are even proposed to be positioned in front of the turbocharger, where also the pressure is significantly higher, up to 5 bar, in addition to the elevated temperatures. Both of these two features would lead to a stronger reduction of pollutant emissions and allow smaller catalytic converters.[6] The optimization of the design and operation conditions of those close-coupled catalysts calls for an analysis of potential homogeneous reactions in the exhaust gas due to the rather high temperature. A very crucial point along these lines is the variation of the NH_3/NO_x ratio due to reactions in the gas phase. In general, the NH_3/NO_x ratio needs to be unity over the entire inlet cross section of the SCR catalyst to avoid either ammonia or NO_x slip; both are not tolerable. Controlling this ratio by adequate dosing of the urea-water solution and additional NH_3 and NO_x storage-release functions of the catalysts used is a great challenge for the NO_x aftertreatment system. Often, ammonia slip catalysts are used in addition, which however lead to the production of significant amounts of N_2O, another greenhouse gas. For all these reasons, it is obvious that the kinetics of homogeneous reactions of NH_3 and NO_x with the other exhaust gas components has to be understood quantitatively, which is the objective of the research study presented here.

There have been only a few studies that deal with the homogeneous reactivity of exhaust gases under those conditions explicitly. Smith et al[7] studied the homogenous chemistry in lean-burn exhaust mixtures of internal combustion engines at moderate temperatures, realizing that NO is converted rapidly to NO_2, whereas HCs are oxidized without a catalytic converter. Torkashvand et al[8] recently found a promotion of the homogeneous oxidation of light alkanes such as CH_4 by NO_x, which also lead to the additional formation of formaldehyde on a level similar to the amount of HCHO in the engine's raw emissions. Günter et al[9] realized that the performance of SCR catalysts can be significantly influenced at elevated temperature and pressure by homogeneous gas phase reactions due to NO and NH_3 oxidation.

The homogeneous reactivity of the respective $NH_3/NO/O_2$ mixtures have been investigated in detail both experimentally and numerically.[10–15] In some of

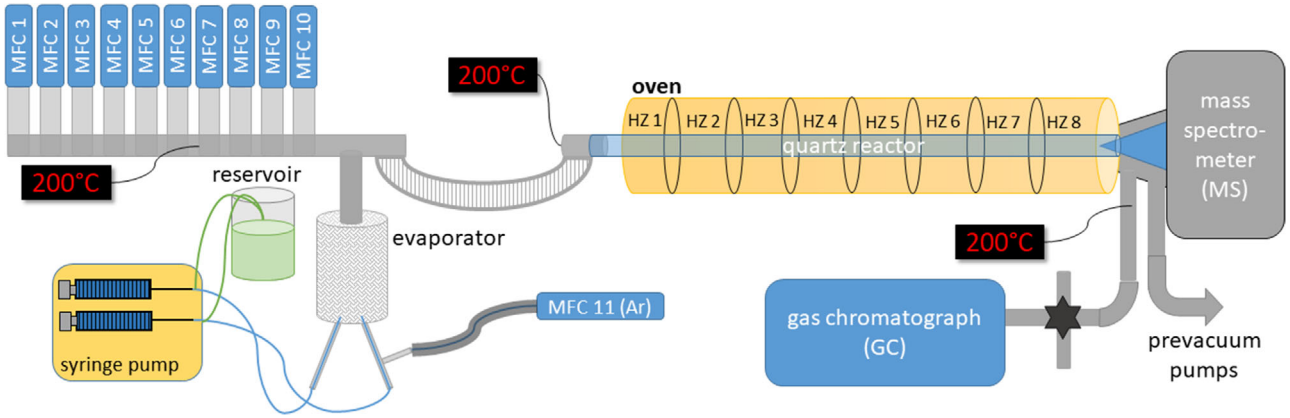

FIGURE 1 Scheme of the plug-flow reactor (PFR) used in this work [Color figure can be viewed at wileyonlinelibrary.com]

these studies, the impact of CO and H_2O on the reactivity was considered. The so-called Thermal $DeNO_x$ process only works in a narrow temperature range from 900 to 1 400 K, whereas additives such as CO shift the specific NO reduction window toward lower temperatures.[16–18] The kinetic models available were mostly developed for these thermal $DeNO_x$ conditions. However, these homogeneous gas-phase reaction mechanisms have not been applied to the best of our knowledge to support the understanding and explain the experimental results of the impact of small HCs on the homogeneous conversion of NO_x and NH_3 at the specific conditions occurring in the exhaust-gas of lean operated natural gas engines, that is, moderate temperatures (for combustion systems), low concentrations of the reactants, and rather long residence times.

In this work, we experimentally and numerically study the effect of the small HCs CH_4, C_2H_4, and additionally CO on the reactivity of NO_x and NH_3 in the gas phase under these conditions. Therefore, we used a plug-flow reactor (PFR) coupled to electron ionization molecular-beam mass spectrometry (EI-MBMS) to investigate five gas mixtures (GMs), starting from $NH_3/NO/O_2$ and subsequently adding NO_2, CH_4, CO, and C_2H_4. The chosen concentrations are close to realistic exhaust GMs of lean burn natural gas engines,[4] and the successive addition of one species at a time allows to individually study the effects of these species on the NH_3/NO reactivity. The experimental results were then analyzed by kinetic simulations using three different kinetic models from literature, which we refer to as CRECK,[19–21] Glarborg,[16] and Konnov.[22] These mechanisms were developed for high and low temperature HC combustion processes such as the thermal $DeNO_x$ including the NO_x chemistry with important HC-nitrogen interaction reactions.

The objectives of this study are twofold: first, the significance of potential gas phase reactions in the presence of the common exhaust components CH_4, CO, and C_2H_4 on the NO_x and NH_3 concentrations in the exhaust-gas pipe is revealed; second, the prediction capability of three established reaction mechanisms is analyzed for these exhaust-gas relevant conditions.

2 | EXPERIMENTAL

All measurements were performed in a PFR at Bielefeld University. The system, the main features of which have been described in detail previously,[23,24] was modified slightly regarding preheating and exhaust gas heating to prevent formation of explosive ammonia nitrate. A scheme of the modified PFR is shown in Figure 1.

All gas flows were controlled by calibrated mass flow controllers (MKS Instruments, 5% uncertainty), mixed within a preheated (473 K) gas line and then guided into the PFR. The PFR consists of a heated fused silica tube (7.26 mm diameter, 130 cm length) where a quartz nozzle (100 μm orifice diameter) is placed at the end used for sampling via a two-stage expansion (1st stage ~10^{-4} mbar, 2nd stage ~10^{-6} mbar). Samples then undergo electron ionization and are analyzed by a time-of-flight mass spectrometer with a mass resolution of $m/\Delta m$ ~2 000. The experiments were performed at 970 mbar in the temperature regime from 700 to 1 200 K. To ensure plug-flow conditions, a total gas flow rate of 0.5 slm was chosen, which is supported by 2D simulations (see Figure S1 in Supplemental Material 1 (SM1)). This total gas flow leads to residence times between 1.5 and 2.4 s, depending on reactor temperature.

The inlet mole fractions of the investigated GMs are summarized in Table 1. All gases were obtained from Linde AG with purities > 99.5 %. To achieve higher accuracy in the experimental compositions despite the low inlet concentrations, NH_3, NO, NO_2, C_2H_4, and CO were added as

TABLE 1 Experimental conditions for the plug-flow reactor experiments

	Inlet mole fraction							
Gas mixture	Ar	O_2	NH_3 (ppm)	NO (ppm)	NO_2 (ppm)	CH_4 (ppm)	C_2H_4 (ppm)	CO (ppm)
GM1	0.939	0.06	1 000	1 000	–	–	–	–
GM2	0.939	0.06	1 000	800	200	–	–	–
GM3	0.937	0.06	1 000	800	200	3 000	–	–
GM4	0.934	0.06	1 000	800	200	3 000	–	1 000
GM5	0.936	0.06	1 000	800	200	3 000	200	–

diluted mixture (typically 0.5%-5%) of the respective gas in argon (Linde AG, ±2% relative uncertainty).

The data evaluation mainly follows procedures described in Ref. 25. Calibration factors relative to argon were obtained from the elemental balance for main species including reactants and products. Direct calibration was performed for most detected intermediates. Information on the respective calibration method used for a certain species is given in Table S1 in SM1. Since low reactant concentrations were necessary to perform experiments close to pre-turbine conditions, a significant influence of background signals was observed. This was considered by temperature-dependent background measurements and correction methods described in SM1 (see Figure S2) and summarized in Table S2. The resulting experimental uncertainties are about 30%. Absolute uncertainties in temperature control are ±15 K, which are relevant when comparing experimental results with kinetic simulations. When comparing different GMs, a relative temperature error of only about ±5 K based on repeated measurements with identical conditions needs to be considered. A complete set of all quantitative species profiles is given in SM2.

3 | KINETIC MODELING

Numerical simulations were performed using the software packages Cantera,[26] CHEMKIN Pro,[27] and DETCHEM.[28] Since there is no dedicated PFR code available in Cantera,[26] the PFR was simulated using a *ReactorNet* of *ConstPressureReactors* (constant pressure 0-dimensional reactors). Integral reaction flow analyses as well as sensitivity analyses were performed using the batch code in CHEMKIN Pro software, whereas simulations of the reactor flow conditions and the NO/NO_2 equilibrium were performed using $DETCHEM^{CHANNEL}$ and $DETCHEM^{EQUIL}$ codes. The temperature profile of the present flow reactor was obtained by an empiric equation based on direct temperature measurements (compare Figure S3 in SM1). This experimental temperature profile was considered in Cantera by using a concatenation of more than 650 reactor segments, which was seen to be a sufficiently high number to obtain an asymptotic invariance to the number of reactor segments. Pre-reactions were considered exemplarily for GM2 and found to be insignificant for the present highly diluted conditions (see Figure S4 in SM1). Three detailed kinetic models from literature were used in their latest original versions including low-temperature chemistry for NO_x and HCs. The Konnov mechanism[22] is developed for modeling combustion processes of hydrogen, carbon monoxide, formaldehyde, carbon monoxide, formaldehyde, methanol, methane, C_2-C_3 HCs, and their oxygenated derivates including H/C/N/O reactions for in-flame NO_x formation and reburning. The mechanism contains 129 species. The CRECK mechanism[19–21] includes pyrolysis, partial oxidation, and combustion of HC and oxygenated fuels. The complete mechanism is developed for the high- and low-temperature kinetics for C_1-C_{16} HCs including a NO_x reaction scheme and contains overall 537 species. The Glarborg mechanism[16] is developed for C_1-C_2 HC, amine, and cyanide chemistry as well as HC-nitrogen interactions. The model contains 151 species and includes detailed nitrogen chemistry. All three mechanisms are validated over a wide range of conditions.

4 | RESULTS AND DISCUSSION

Figure 2 shows the experimental and predicted mole fraction profiles of the main species for the five GMs. The NH_3/NO and NH_3/NO_x reactivity is studied upon addition of NO_2 (GM2), CH_4 (GM3), CH_4/CO (GM4), and CH_4/C_2H_4 (GM5). The agreement between experimental and simulation results using the three kinetic models is reasonably good for all five GMs. However, some smaller deviations can be observed between experiments and simulations, but also between the different kinetic models.

In the following sections, we will first analyze the fundamental NH_3/NO_x system (Section 4.1) and then discuss the influence of HCs and CO (Section 4.2) followed by an investigation of the NH_3/NO_x ratio which is crucial for the functionality of SCR catalysts (Section 4.3).

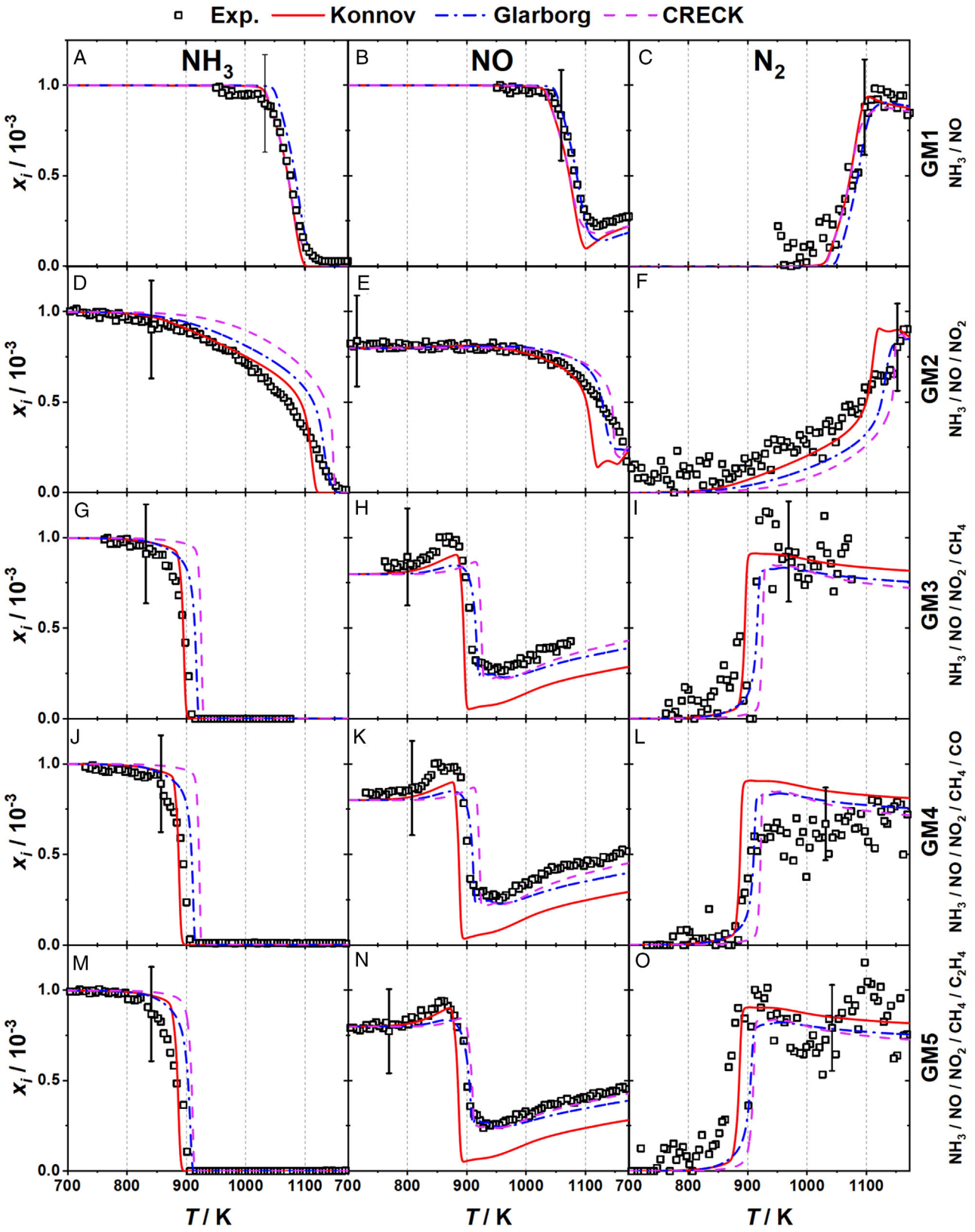

FIGURE 2 Experimental mole fraction profiles (symbols) for NH_3 (left), NO (center), and N_2 (right) for the investigated gas mixtures (GM) compared with simulation results (lines). The experimental uncertainty of 30% is indicated at only one temperature for clarity [Color figure can be viewed at wileyonlinelibrary.com]

4.1 | Kinetic analysis for $NH_3/NO_x/O_2$ mixtures

In the NH_3/NO system (GM1), the onset temperature of NO and NH_3 is near 1 020 K (Figures 2A–2C). The agreement of experimental and predicted results using the three kinetic models is overall good. However, the Konnov and the CRECK mechanisms show conversion of NO and NH_3 at slightly lower temperatures compared with the Glarborg mechanism by approximately 10 K. N_2 is the main product of this reaction, which is also predicted reasonably well by the models (Figures 2C, 2F, 2I, 2L, and 2O). Nevertheless, a larger scatter is observed in the experimental N_2 mole fraction profile for the HC-containing GM3-GM5 (Figures 2I, 2L, and 2O), since the presence of CO makes it harder to extract a clear N_2 signal from the experimental data due to the small mass difference (0.011 u). At 1 100 K, the Konnov mechanism predicts the highest NH_3 conversion of 99% and the highest N_2 formation, whereas lower conversion can be found using the Glarborg and the CRECK mechanisms. The reduction of NO by NH_3 in the basic $NH_3/NO/O_2$ mixture has been studied extensively before, both experimentally and numerically, and is well known as SNCR with NH_3 (thermal $DeNO_x$).[16–18,29–34] The thermal $DeNO_x$ process only works in a narrow temperature range from 1 100 to 1 400 K and excess oxygen.[16,18,29] Additives such as $H_2/CO/CH_4$[18,35–37] shift the temperature window to lower temperatures, whereas H_2O has a slightly inhibiting effect.[16,18,36] While the binary mixtures of, for example, NH_3+NO or NO+O_2 are inert, the thermal $DeNO_x$ process works due to chain branching reactions allowing the overall reaction being self-sustaining.[18] Therefore, NH_3 is oxidized by the O/H radical pool, primary OH radicals producing NH_2 which further reacts with NO via two major reaction pathways; one radical producing (R1) and the other chain terminating (R2).[16,18] The required branching ratio of reactions (R1) and (R2) is defined as $\alpha = k_{R1}/(k_{R1} + k_{R2})$ with typical values of $\alpha = 0.3\text{-}0.4$ (1 100-1 400 K).[16]

$$NH_2 + NO = NNH + OH \quad (R1)$$

$$NH_2 + NO = N_2 + H_2O \quad (R2)$$

Above 1 100 K, NO conversion is reduced, which is typical for the thermal $DeNO_x$ process due to increasing chain carrier concentrations such as OH and O radicals. Therefore, NH_2 reaction pathways via NH_2 + NO, which subsequently lead to NO conversion, compete with reaction pathways with the O/H radical pool via $NH_2 + OH = NH + H_2O$ and NH_2+O = HNO + H, leading to NO formation.[18]

In contrast to the thermal $DeNO_x$ process, highly diluted conditions at moderate temperatures were studied here. A sensitivity analysis was performed at 1 040 K confirming that reaction (R1) is the most sensitive reaction found for both NH_3 and NO conversion. A reaction flow analysis for GM1 is provided in SM1 (Figure S5). The calculated branching ratios α are in the recommended range for the Thermal $DeNO_x$ process. Figure 3 shows an Arrhenius plot comparing the rate coefficients k_f for reaction (R1). The origin of the corresponding Arrhenius parameters for reaction (R1) are summarized in Table S3 with calculated k_{R1} and α values at 1 100 K, respectively. The lowest rate coefficient k_f and therefore slower reaction kinetic was found for the Glarborg mechanism which is in accordance with the NH_3 consumption onset shifted slightly toward higher temperatures as shown in Figure 3B. As already discussed by Glarborg et al,[16] small changes to the branching ratio can lead to a shift of onset temperature by 20-50 K.

To underline the importance of the aforementioned reaction and its impact on NH_3 and NO conversion at the highly diluted conditions studied here, the Glarborg mechanism was tentatively modified by increasing the pre-exponential factor A and the temperature coefficient β independently. Both changes led to a higher k_f value and therefore a higher branching ratio indicating a faster reaction of (R1). The impact of this slight modification is visualized in Figure 3A. The k_f values calculated with the Arrhenius parameters from the original Glarborg mechanism are shown as solid dark blue line, whereas the tentatively modified Arrhenius parameters leading to k_f values are presented as a light blue dashed-dotted line. In Figure 3B, the simulation of GM1 was repeated with the adjusted temperature coefficient leading to an earlier conversion compared with the results obtained with the original Arrhenius parameters from the Glarborg mechanism, which agrees better with the experimental data and the simulation results obtained with the CRECK and Konnov mechanisms in Figure 2.

In GM2, NO was partially replaced by NO_2, keeping the overall NO_x concentration constant (see Table 1). The chosen NO/NO_2 ratio of 4:1 is representative for natural gas engine conditions.[4,38] Nitrogen dioxide (NO_2) is believed to be a key intermediate in the thermal $DeNO_x$ process.[16] The modeling predictions for the NO_2 produced at thermal $DeNO_x$ conditions are according to Glarborg et al[16] in qualitative agreement with measured ones; however, the predicted NO_2 temperature window was extended to higher temperatures, which was not observed experimentally according to Ref. 16. The formation sequence of NO_2 through competitive reactions of HNO and H_2NO with the radical pool are not well characterized but important to predict NO_2 consumption/formation correctly.[16] This might be also important because to the authors'

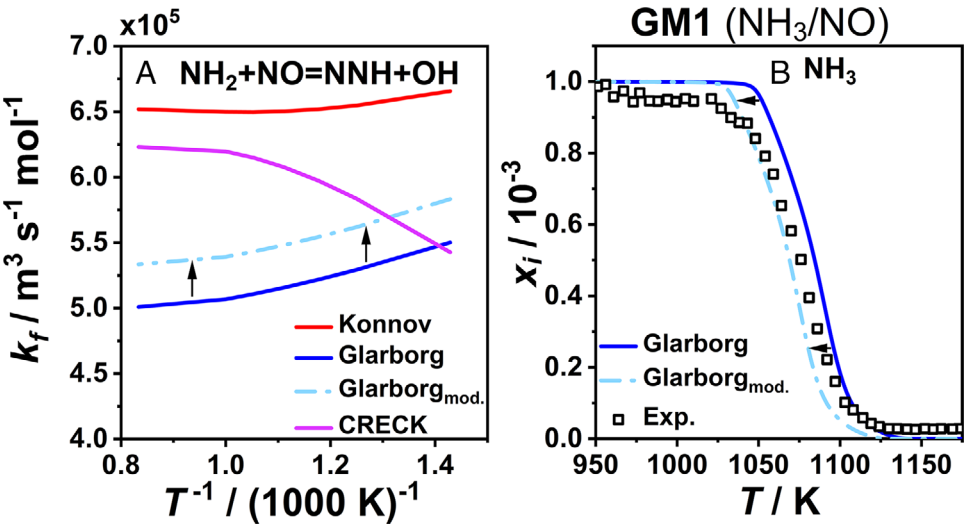

FIGURE 3 (A) Arrhenius plot for the reaction (R1) with the Arrhenius parameters from the Konnov (red solid line), Glarborg (dark blue solid line), and CRECK (purple solid line) mechanisms. The light blue dashed-dotted line denotes the k_f values with modified Arrhenius parameters (adjusted β value) for the Glarborg mechanism. (B) Species mole fraction profile of NH_3 simulated for GM1 with the original and tentatively modified Glarborg mechanism [Color figure can be viewed at wileyonlinelibrary.com]

knowledge, the role of both NO and NO_2 in the feed gas as comparable to the exhaust gas of natural gas engines was not investigated before.

Similar to the NH_2 + NO reaction channels (R1) and (R2), two further reaction pathways are according to the literature[16] important at large excess oxygen due to NO_2 formation via $NO + HO_2 = NO_2 + OH$. Again, one is chain terminating (R3) and the other one is radical producing (R4). The radical producing path (R4) forms NO via the reaction sequence $NO_2 \rightarrow H_2NO \rightarrow HNO \rightarrow NO$.

$$NH_2 + NO_2 = N_2O + H_2O \quad (R3)$$

$$NH_2 + NO_2 = H_2NO + NO \quad (R4)$$

As can be observed in Figures 2D–2F, NH_3 conversion starts about 200 K and NO conversion about 50 K earlier compared with GM1. For both species, the mole fraction profiles of GM2 are flatter compared with the mole fraction profiles of GM1. The flatter shape must be directly correlated to the NO_2 addition in the feed gas. Figure 4 shows a reaction path analysis performed for GM2 at 1 040 K. This temperature was chosen to see direct differences in reaction pathways due to NO_2 addition compared with GM1 (Figure S4), which was also performed at 1 040 K. The major reaction paths also important for GM1 are shown with solid arrows, whereas the additional reaction paths important due to NO_2 addition in the feed gas are denoted with dashed arrows. In the NH_3/NO GM, NH_3 is mainly oxidized by OH radicals, whereas NH_3 can additionally be oxidized by inlet NO_2 in GM2. The NO_2 addition in the feed gas seems to allow for different reaction pathways producing important radicals which enhance, for example, NH_3 conversion at low temperature.

According to the NO/NO_2 equilibrium (Figure S6), NO_2 is converted to NO with increasing temperature. However, no increase in NO mole fraction can be observed at temperatures below 1 000 K (Figure 2E) and NO consumption starts significantly later compared with NH_3 (Figure 2E). At the same time, an increase of N_2 was measured experimentally above 800 K and is confirmed by simulation results (Figure 2F). These observations suggest that the formed NO via the NO/NO_2 equilibrium and reaction (R4) must be rapidly consumed via reaction (R1) so that no NO conversion can be observed experimentally and numerically below 1 000 K. A sensitivity analysis is shown in Figure 5A for NO and Figure 5B for NH_3 at 1 040 K. NO is formed via the NO/NO_2 equilibrium and reaction (R4), which was found to be sensitive. According to the mole fraction profile, NO must be directly consumed, possibly via reaction (R1) ($NH_2 \rightarrow NNH \rightarrow N_2$), which was again found to be most sensitive for NO and NH_3 consumption in all three kinetic models producing N_2, whereas quantitative influences are seen to differ for most reactions (Figure 5).

The shapes of NH_3 and NO species mole fraction profiles differ from the experimentally measured ones, especially at higher temperatures (Figures 2D–2F). This might indicate that the importance of NO_2 as reactant (NO/NO_2 equilibrium) and its intermediate species formed are underestimated at temperatures above 1 050 K in all three kinetic models. It can be concluded that the presence of NO_2 in the feed gas has a retarding effect on NO conversion (Figure 2E) and hence a negative impact on

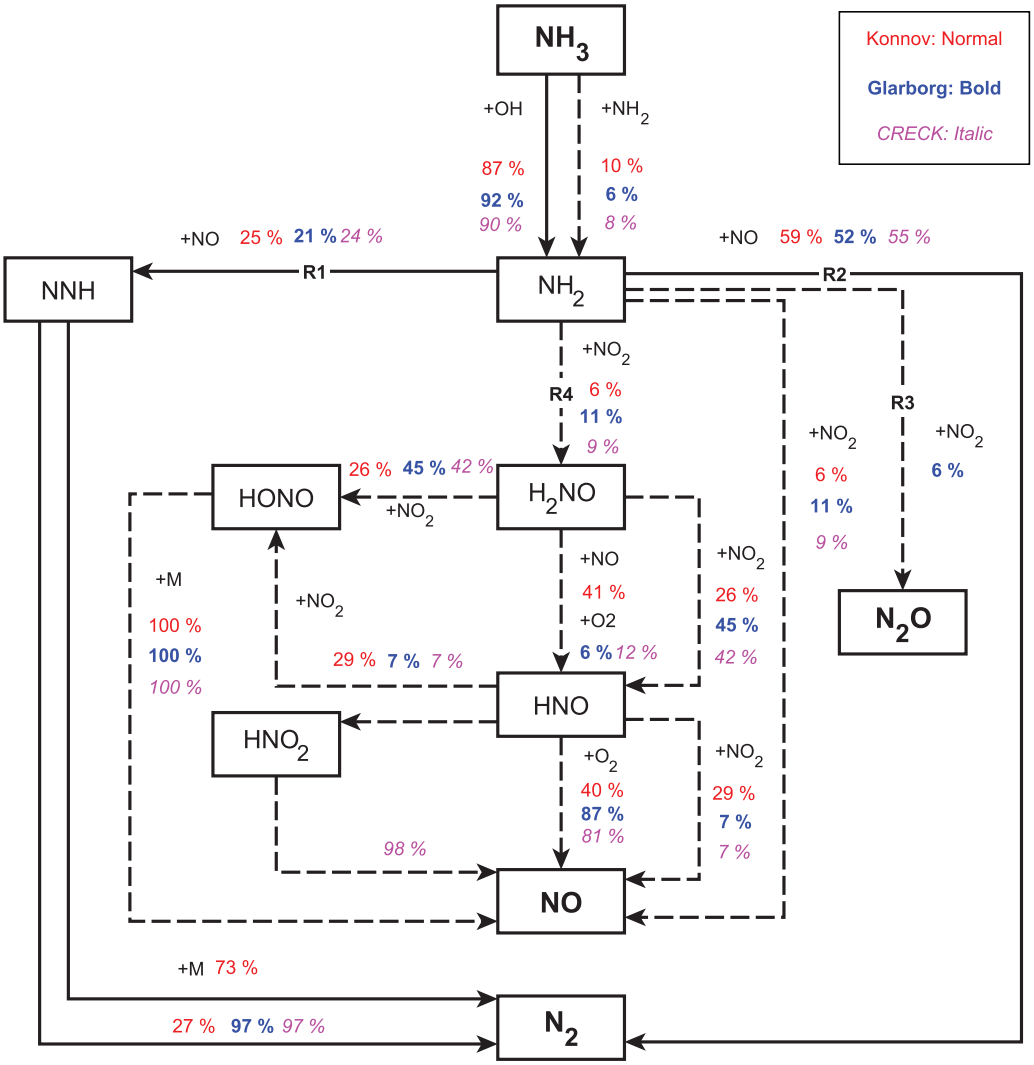

FIGURE 4 Major reaction pathways at 1 040 K in the oxidation of NH_3 for GM2. The solid arrows indicate the major reaction pathways of GM1 and additional pathways due to NO_2 addition are denoted with dashed arrows. Simulations with the Konnov (normal), Glarborg (bold), and CRECK (italic) mechanisms [Color figure can be viewed at wileyonlinelibrary.com]

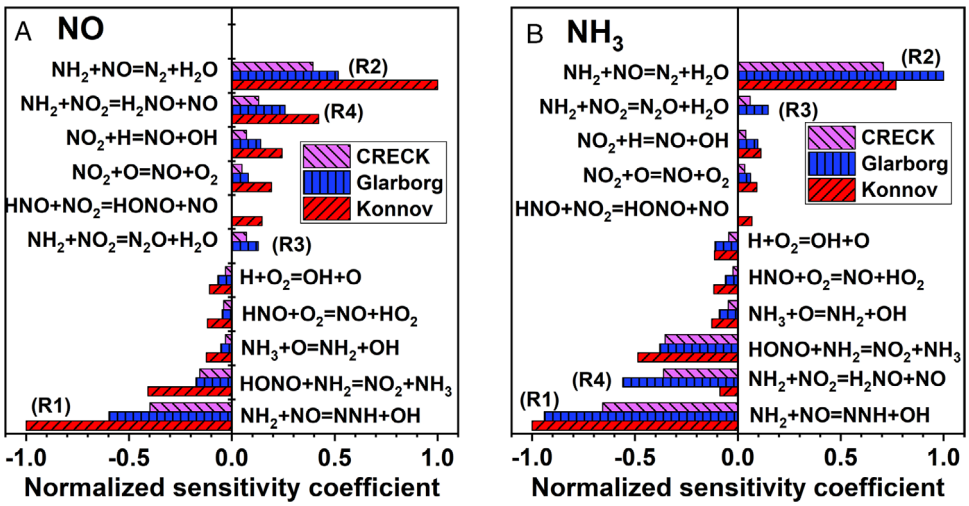

FIGURE 5 Sensitivity analysis for (A) NO and (B) NH_3 at 1 040 K with the Konnov, Glarborg, and CRECK mechanisms [Color figure can be viewed at wileyonlinelibrary.com]

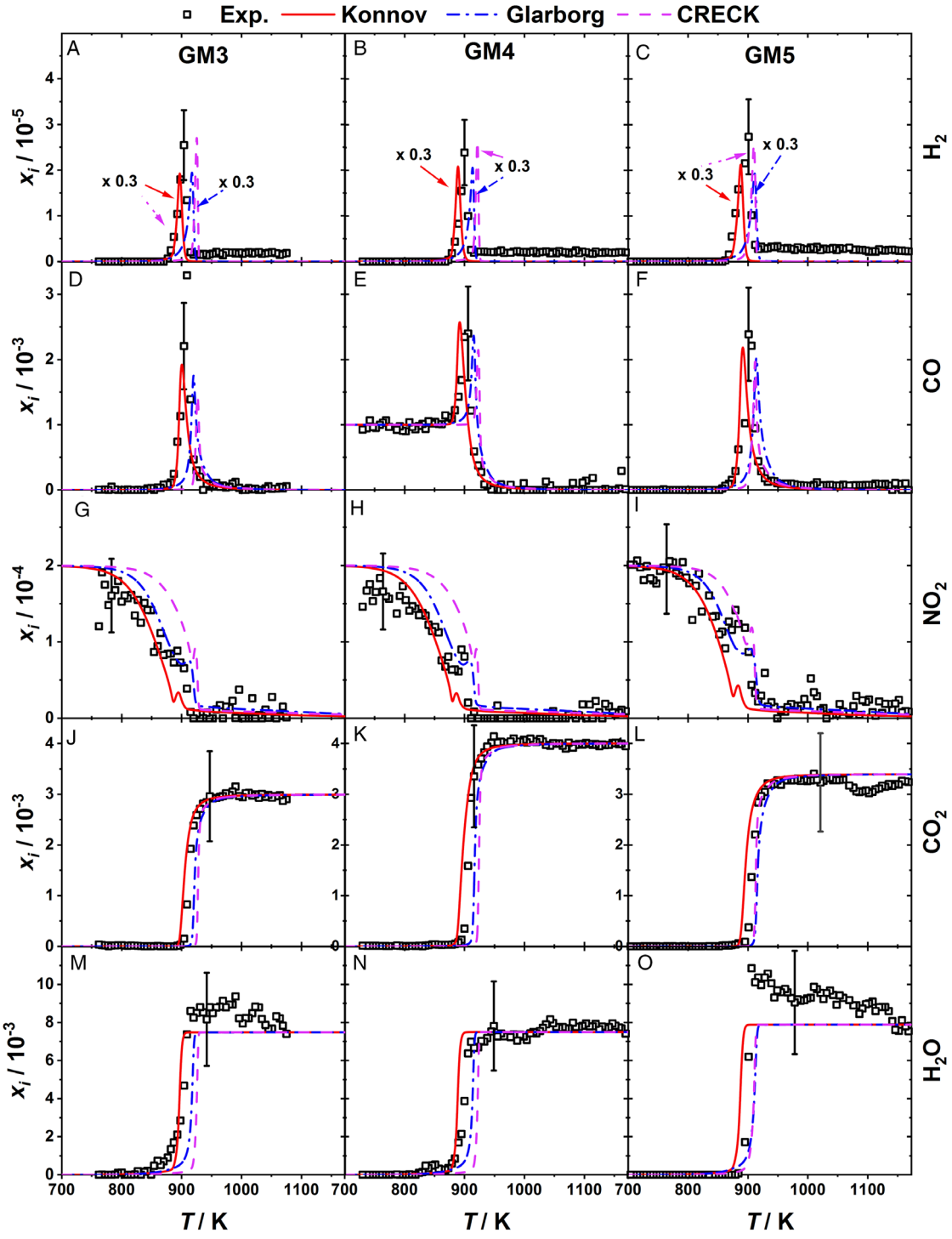

FIGURE 6 Experimental mole fraction profiles (symbols) for H_2, CO, NO_2, CO_2, and H_2O of different investigated gas mixtures (GM) in PFR experiments compared with kinetic simulations (lines). The experimental uncertainty of 30% is indicated at only one temperature point for clarity [Color figure can be viewed at wileyonlinelibrary.com]

exhaust-gas aftertreatment of combustion processes. Using these kinetic models at, for example, natural gas engine conditions, work needs to be done clarifying the role of both NO and NO_2 as reactant in the feed gas by studying the important intermediate species such as H_2NO and HNO which are important for the NH_3/NO_X reactivity.

4.2 | Kinetic analysis of CO, CH_4, and C_2H_4 addition

GM3-GM5 all contain additional HC species representative for natural gas engines,[4,38] namely CH_4, CO, and additionally C_2H_4 in lesser amounts in GM5. These species

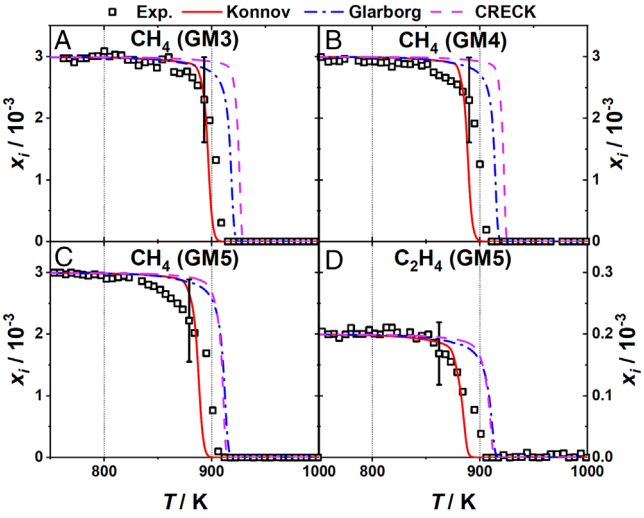

FIGURE 7 Experimental mole fraction profiles (symbols) for CH_4 and C_2H_4 for the investigated gas mixtures (GM) compared with simulations (lines). The experimental uncertainty of 30% is indicated at only one temperature for clarity [Color figure can be viewed at wileyonlinelibrary.com]

decrease the temperature of NH_3 total conversion and NO_x significantly by nearly 300 K compared with GM2 (Figure 2). In GM3-GM5, no major differences in main species mole fraction profiles can be observed. Mole fraction profiles of selected intermediates and products are shown in Figure 6. NO_2 consumption (Figures 6G–6I) starts already below 780 K, whereas NH_3 conversion starts at 877 K (Figures 2G, 2J, and 2M) followed by CH_4 at 893 K (Figures 7A–7C) and NO latest at 904 K (Figures 2H, 2K, and 2N) due to NO formation below 900 K. Adding C_2H_4 in GM5 (Figures 7C and 7D) shifts the onset temperature of HC again about 10 K toward lower temperature. The overall agreement of experimental and simulation results is reasonably good for the three kinetic models. Nevertheless, the Konnov mechanism overpredicts the NO conversion as already observed for GM2 (Figure 2E). Furthermore, it can be observed for the Konnov mechanism that NO is produced in significant amounts around 850 K, and rapidly consumed at 900 K. These trends are also predicted with the Glarborg and CRECK mechanisms but less pronounced and shifted to higher temperatures. At maximum NH_3/NO conversion, CO (Figures 6D–6F) and intermediate species such as CH_2O, which will be discussed later (Figure 11), peak at 900 K as well as NO_2. GM4 and GM5 show rather similar profiles compared with GM3 (Figures 2G–2O). This can be underlined by the species mole fraction profiles for H_2, CO, CO_2, H_2O, and NO_2 shown in Figure 6. Only for GM4, the CO_2 mole fraction profile is higher compared with GM3 and GM5 indicating that the added CO is oxidized directly to CO_2.

The decomposition of the HC additives in the fuel mixtures is shown in Figure 7. Again, the three kinetic models can capture the species mole fraction profiles very well. However, the onset with the Glarborg and CRECK mechanisms is shifted about 30 K toward higher temperatures.

The mutual promoting effect of HC/NO,[13,39–41] HC/NO_2,[13,41] and HC/NO_x[42,43] mixtures has been studied extensively before. Investigations of the $CO/NO/NH_3$[37,44] and $CH_4/CO/NO/NH_3$[15] systems remain rather scarce, whereas studies of the whole $HC/CO/NH_3/NO_x$ system containing both HC and NH_3 as reducing agent close to exhaust-gas aftertreatment conditions of natural gas engines are not known. Since simulation results are in quite good agreement with experimental data (Figure 2) at these highly diluted exhaust natural gas conditions, a reaction flow analysis was performed for GM3 as the first mixture containing both N and C species to gain deeper insight into the $HC/NH_3/NO_x$ reaction behavior. For each mechanism, the reaction flow analysis was performed at two temperatures, namely a lower temperature corresponding to an initial, additional 5% NO formation (ie, −5% NO conversion) and the temperature of maximum NO conversion, which is at the same temperature as the CO (Figures 6D–6F) and CH_2O (Figure 11) peak temperature. The maximum NO conversion temperature was chosen because major deviations between the three kinetic models were observed at this temperature (compare Figure 2). In general, major reaction pathways do not differ at these two chosen temperatures except for one aspect. At the maximum NO conversion temperature, all mechanisms have in common that H-abstraction from NH_3 forms NH_2 as major initial step in NH_3 oxidation. At the lower temperature where 5% additional initial NO is formed, however, NH_3 can be additionally reduced by NO_2 in the Konnov and CRECK mechanisms. Since other major reaction pathways do not differ significantly at low and high temperatures, only the reaction flow analysis at the maximum NO conversion temperature is discussed in detail. In Figure 8, the reaction flow analysis is shown for the $NH_3/NO/NO_2$ species consumption in GM3 at both temperatures for each mechanism. The direct interaction of HC/N species is highlighted by reacting HC species written in bold italic characters next to the arrows.

The H-abstraction from NH_3-forming NH_2 radicals was found as initial step in NH_3 oxidation in all three mechanisms. The produced NH_2 radicals are mainly consumed by reactions (R1) and (R2) that were also found to be the major NO reduction pathways for GM1 and GM2 (Figure S4). Around 900 K, the direct oxidation pathway of NH_3 with NO_2 is of minor importance; however, the reaction between NH_2 and NO_2 might be crucial for NO formation. Comparing the experimental data with the three kinetic models, it is obvious that the Konnov mechanism

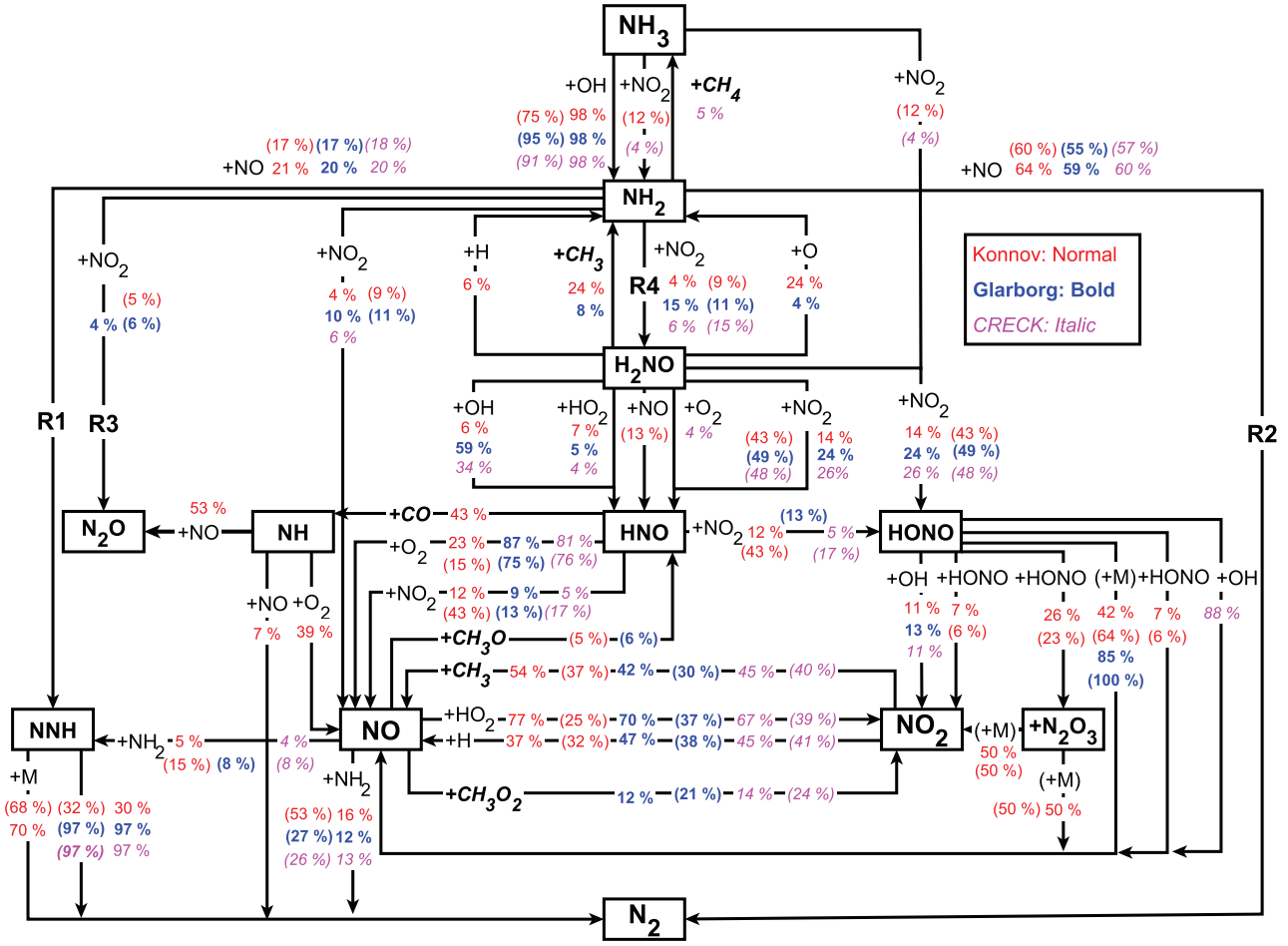

FIGURE 8 Major reaction pathways for NH_3/NO/NO_2 consumption in GM3. The interacting HC species are written above the arrows highlighted by bold italic letters. Simulations were performed at the temperature where an initial, additional amount of 5% NO is formed (−5% NO conversion, shown in brackets) with the Konnov (normal, red, $T = 834$ K), Glarborg (bold, blue, $T = 866$ K) and CRECK (italic, purple, $T = 894$ K) mechanisms as well as at maximum NO consumption temperature with the Konnov (normal, red, $T = 900$ K), Glarborg (bold, blue, $T = 920$ K), and CRECK (italic, purple, $T = 926$ K) mechanisms [Color figure can be viewed at wileyonlinelibrary.com]

overpredicts the maximum NO conversion (Figure 2H). The reaction sequence $NH_2 \rightarrow H_2NO \rightarrow HNO \rightarrow NO$ due to the availability of NO_2 is rather underrepresented in the Konnov mechanism, which could be a possible explanation. Conversely, compared with the Glarborg and CRECK mechanisms, additional reaction pathways such as the oxidation of HONO via $HONO \rightarrow N_2O_3 \rightarrow NO/NO_2$ were found as well as HNO reduction via the reaction sequence $HNO \rightarrow NH \rightarrow N_2O \rightarrow N_2$, effectively leading to NO reduction.

In general, NO consumption in this mixture seems to be achieved by the competitive NO oxidation reactions toward NO_2 by CH_3O_2 (R5) and HO_2 (R6) according to the reaction flow analysis for all three kinetic models.

$$CH_3O_2 + NO = CH_3O + NO_2 \quad \text{(R5)}$$

$$NO + HO_2 = NO_2 + OH \quad \text{(R6)}$$

This does not seem surprising since these reaction pathways were already identified as the most important NO oxidizing pathway at low temperature HC oxidation in mixtures doped with NO.[39,40] The promoting effect of NO on HC oxidation was traced back to the formation of chain carriers such as CH_3O and CH_3O_2 radicals, which are no longer chain terminating due to the addition of NO. This finding can be transferred to the present study, since HC radicals promote NO_x and NH_3 consumption.

In Figure 9, a reaction flow analysis for CH_4 oxidation is shown with all three kinetic models performed at 5% NO formation (ie, −5% NO conversion) shown in brackets and maximum NO conversion temperature. No differences were observed in major reaction pathways therefore only the reaction flow analysis at maximum NO conversion temperature is discussed in the following. Important nitrogen species are written above the arrows in bold, italic letters. The CH_3O and CH_3O_2 radicals are formed by CH_3

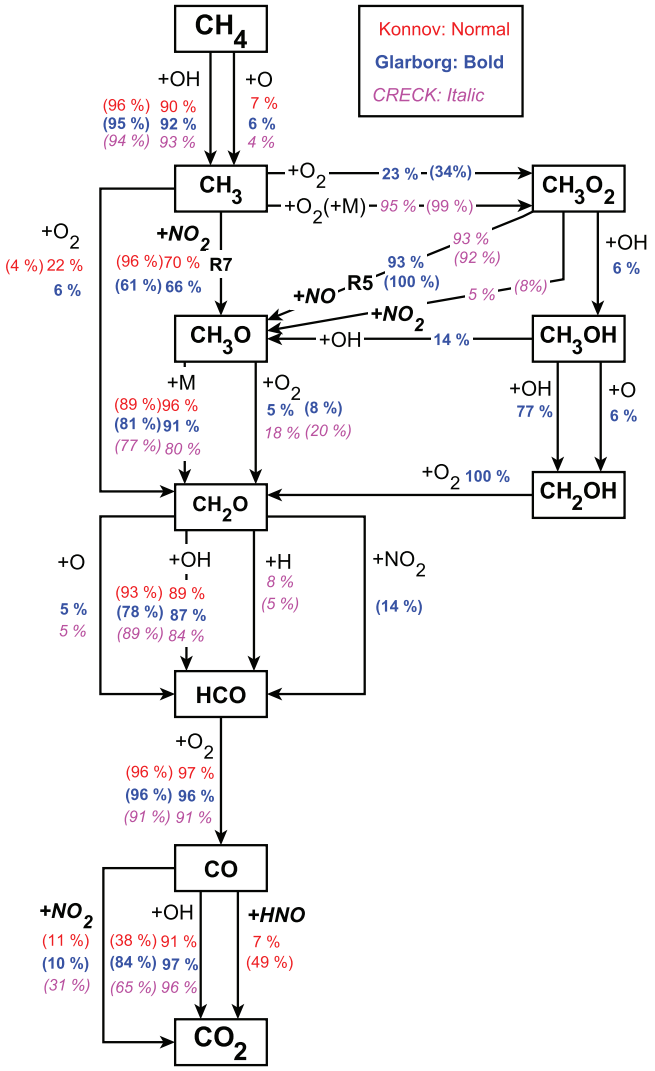

FIGURE 9 Integral reaction flow analysis of CH_4 oxidation pathways for GM3. Simulations were performed at the temperature where an initial, additional amount of 5% NO is formed (−5% NO conversion, shown in brackets) with the Konnov (normal, red, $T = 834$ K), Glarborg (bold, blue, $T = 866$ K), and CRECK (italic, purple, $T = 894$ K) mechanisms as well as at maximum NO consumption temperature with the Konnov (normal, red, $T = 900$ K), Glarborg (bold, blue, $T = 920$ K), and CRECK (italic, purple, $T = 926$ K) mechanisms [Color figure can be viewed at wileyonlinelibrary.com]

oxidation with NO_2 (R7) and O_2, whereas the latter is of minor importance due to high energy barrier,[40] concluding that the methyl radicals are the most important interacting HC-/N-species.

$$CH_3 + NO_2 = CH_3O + NO \quad \text{(R7)}$$

$$CH_3NO_2 + [M] = CH_3 + NO_2 \quad \text{(R8)}$$

In addition, reaction (R8) is also discussed in the literature,[13,39] which is particularly important for low temperature HC oxidation in which CH_3NO_2 is produced and competes with reaction (R7). However, this species was not found to have a significant impact on the NO_x/NH_3/HC reactivity in the reaction flow analysis and was not detected experimentally, possibly due to the highly diluted conditions in the present study.

The importance of CH_3 and therefore CH_3O radicals can be underlined by a reaction flow analysis for CH_3O radicals shown in Figure 10 performed at 920 K using the Glarborg mechanism. The reactions (R7) (#932) and (R5) (#968) with NO/NO_2 as oxidizing species are most responsible for CH_3O radical formation, whereas CH_3O radicals are consumed by oxidation reactions, producing CH_2O as intermediate species of partial HC oxidation.

The dehydrogenation of CH_3O toward CO_2 via the reaction sequence $CH_3O \rightarrow CH_2O \rightarrow HCO \rightarrow CO \rightarrow CO_2$ then also contributes to the OH radical pool. Also, for OH radicals, the major formation/consumption pathways are shown in Figure 10. The OH radical formation is mainly driven by NO/NO_2 interchanging reactions (#728, #730) such as reaction (R6). Major consumption pathways of OH radicals are HC oxidation reactions such as $CH_4 + OH$ (#68), $CH_2O + OH$ (#50), and $CO + OH$ (#29). The formation of the intermediate species CH_2O is mainly by oxidation of CH_3 via the reaction path $CH_3 \rightarrow CH_3O_2/CH_3O \rightarrow CH_2O$, whereas its consumption is mainly via the reaction sequence $CH_2O \rightarrow HCO \rightarrow CO \rightarrow CO_2$. Formaldehyde is not only an important intermediate in CH_4 combustion but also crucial regarding possible emissions of natural gas engines because of its toxicity and carcinogenicity. Simulated mole fraction profiles of CH_2O are shown in Figure 11, which are compared with normalized signals of CHO. Due to the very small mass difference between CH_2O and NO of only 0.013 u, a possible CH_2O signal is overlapped with the stronger signal of NO. However, a signal of CHO at $m/z = 29$ u was detected and corrected for isotopes ($^{15}N^{14}N$ and $^{13}C^{16}O$). CHO is a very prominent fragment of CH_2O in EI-MBMS, and therefore the normalized CHO signal can be considered directly proportional to the CH_2O mole fraction. Similar profile shapes are observed in Figure 11 in the experiment and for the Konnov, Glarborg, and CRECK mechanisms. Consistent with the HC consumption results in Figure 7, the maximum CHO signal is observed at nearly identical temperatures of about 890 K for GM3 and GM4, whereas the maximum for GM5 is detected at a lower temperature of about 870 K. Maximum formaldehyde mole fractions in the 10^{-4} range can be expected according to the simulations that are non-negligible regarding the share of HCs in the initial GMs. The present results lead to the suggestion that CH_4 dominates the CH_2O formation for all three mixtures, since neither CO nor C_2H_4 addition substantially modify the CH_2O concentration.

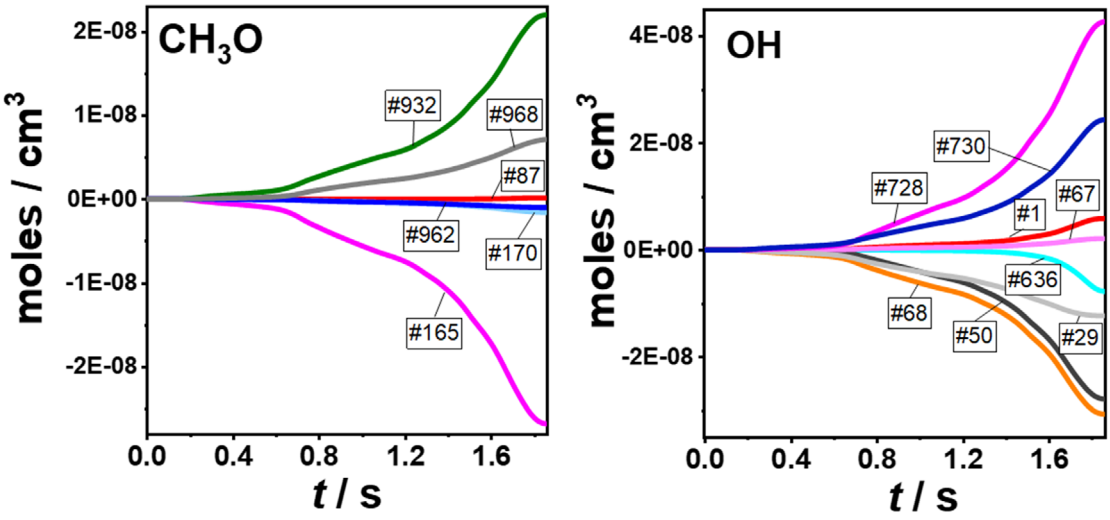

#1: $H+O_2=O+OH$	#87: $CH_3+HO_2=CH_3O+OH$	#730: $NO_2+H=NO+OH$
#29: $CO+OH=CO_2+H$	#165: $CH_3O(+M)=CH_2O+H(+M)$	#932: $CH_3+NO_2=CH_3O+NO$
#50: $CH_2O+OH=HCO+H_2O$	#170: $CH_3O+O_2=CH_2O+HO_2$	#962: $CH_3O+NO=CH_2O+HNO$
#67: $CH_4+O=CH_3+OH$	#636: $NH_3+OH=NH_2+H_2O$	#968: $CH_3O_2+NO=CH_3O+NO_2$
#68: $CH_4+OH=CH_3+H_2O$	#728: $NO+HO_2=NO_2+OH$	

FIGURE 10 Integral reaction flow analysis of CH_3O and OH radical formation/consumption for the Glarborg mechanism at maximum NO conversion at 920 K [Color figure can be viewed at wileyonlinelibrary.com]

Formaldehyde is then further oxidized by the reaction sequence $CH_2O \rightarrow HCO \rightarrow CO \rightarrow CO_2$. Alzueta et al[37] studied a mixture of $CO/NH_3/NO/O_2/H_2O$ experimentally, indicating that the presence of CO affects the radical pool and leads therefore to chain branching reactions but does not contribute directly to NO reduction. As shown in Figure 6, CO peaks at 900 K as well as CO_2 and H_2, whereas the NO consumption starts rapidly. Since in the present study lean mixtures were investigated, CO is oxidized very fast to CO_2 producing important radicals around 900 K and reducing the overall oxygen availability in the system. As already observed for GM2, the NO/NO_2 equilibrium strongly impacts the reaction kinetic of these GMs. At temperatures below 900 K, NO is produced which was observed experimentally and is confirmed by simulation results. Equilibrium calculations in Figure 12 for GM3 show that NO_2 is still present in the GM below 900 K, which can then be reduced by H or CH_3 radicals to NO (see Figure 8). With increasing temperature, the NO/NO_2 equilibrium is then shifted toward NO. Therefore, the equilibrium is not only dependent on temperature but also on oxygen concentration. This leads to the conclusion that if HCs are present in the GM, they will be oxidized very fast to CO and H_2 and further to CO_2, consuming oxygen, which reduces the oxygen availability drastically. This influences the NO/NO_2 equilibrium in shifting it further to lower temperatures allowing the sharp NO consumption profile above 900 K (see Figure 6).

The addition of further HC and C species, namely CO in GM4 and CO/C_2H_4, in GM5 has only minor impact on the NH_3/NO_x reactivity. The impact of CO is in comparison with CH_4 less pronounced; however, the addition of C_2H_4 should have a stronger promoting effect than CH_4.[37,39] This can be observed by a slight temperature shift about 10 K toward lower temperature compared with the addition of CH_4 in GM3 (Figure 7). This only slight temperature shift in GM5 must be due to the lower concentrations and highly diluted conditions. In the present study, it can be concluded that the influence of additional CO (GM4) and minor amounts of C_2H_4 (GM5) on NO_x conversion is significantly lower than the effect of CH_4 addition at highly diluted exhaust-gas aftertreatment conditions.

4.3 | NH_3/NO_x ratio

Since the NH_3/NO_x ratio of one is crucial for SCR catalytic converters to function properly, experimental and simulation results are shown in Figure 13 for GM2 and GM3, respectively. Please note, that the absolute uncertainty of the experimental NH_3/NO_x ratio is shown in

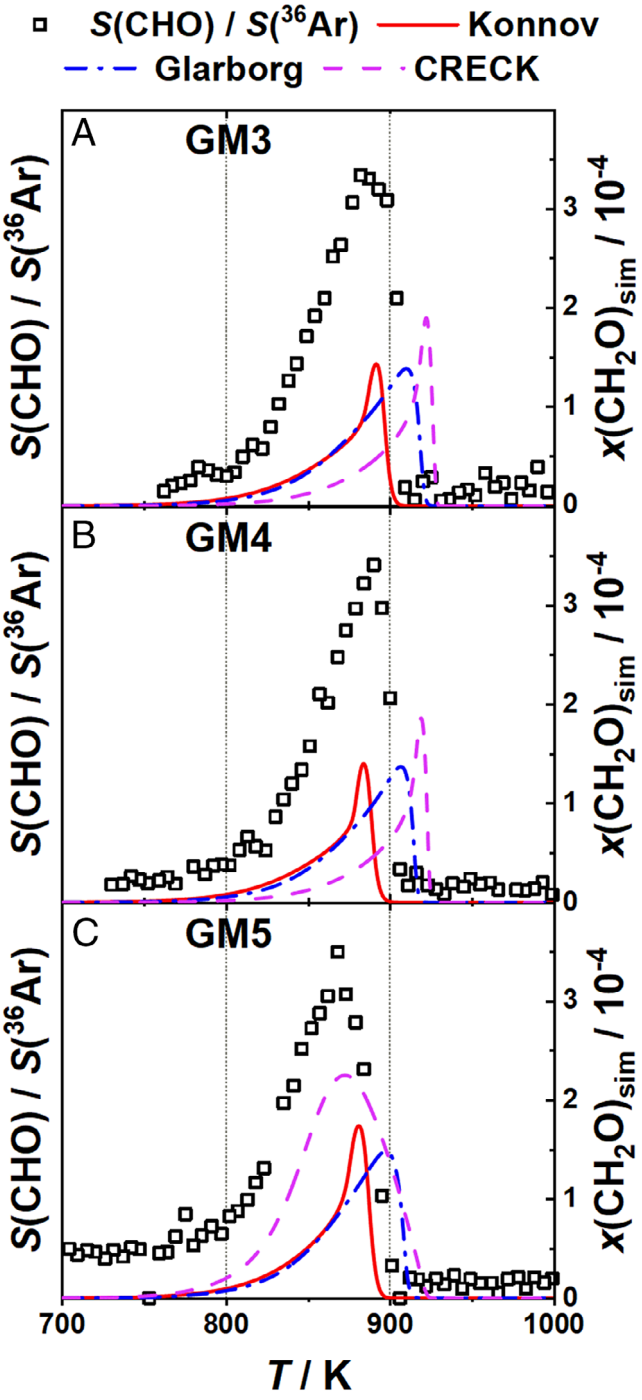

FIGURE 11 Experimental signal profiles of CHO (symbols, left axis) normalized by the argon signal in GM3-GM5; CHO as a fragment of CH_2O is considered as proportional to the CH_2O mole fraction. Simulations for CH_2O are shown for comparison (lines, right axis) [Color figure can be viewed at wileyonlinelibrary.com]

Figure 13 and that the relative error between different measurements is smaller. It can be observed that the NH_3/NO_x ratio changes significantly with increasing temperature, which could lead to undesired emissions. The difference in temperature dependences between NH_3 and NO_x can be represented very well for both GMs with all three kinetic

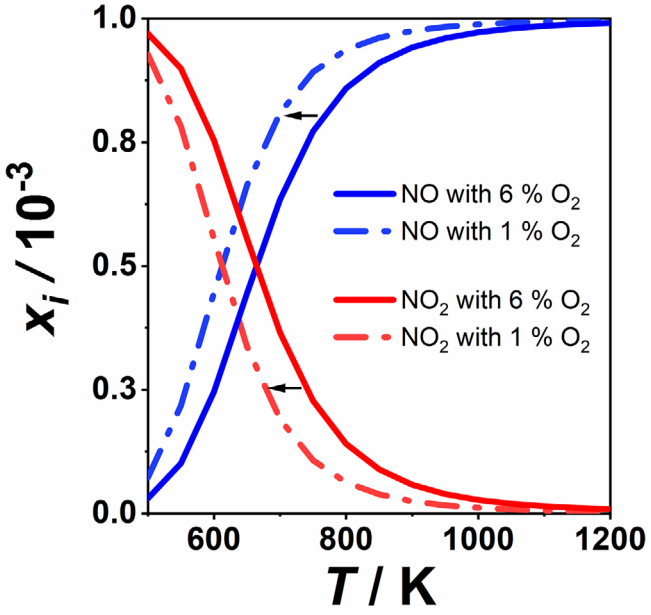

FIGURE 12 NO/NO_2 equilibrium simulated with DETCHEM^{EQUIL} of GM3 (solid lines) and GM3 with 1% oxygen (dashed-dotted lines) [Color figure can be viewed at wileyonlinelibrary.com]

models. Even though these three mechanisms predict the trends quite well, none of them leads to a quantitative agreement in the temperature ranges of 900-1 150 K and 850 and 900 K for GM2 and GM3, respectively. Again, the strong impact of the presence of CH_4 in the exhaust is clearly observed. Since the NH_3/NO_x ratio begins to deviate from unity at rather low temperatures as occurring in the tail pipe close to the engine, it is obvious that homogenous gas phase reactions have to be considered for the development of exhaust gas aftertreatment systems for lean-operated natural gas engines.

5 | CONCLUSION

In this work, the reactivity of the $NO/NH_3/O_2$ system has been studied regarding the influence of NO_2, CH_4, CO, and C_2H_4, which are important components of engine exhaust in lean-operated natural gas engines, that is, in excess of oxygen. Our study combines PFR experiments coupled to EI-MBMS in the temperature range from 700 to 1 200 K with simulations using three well-established kinetic models from the literature, namely CRECK,[19–21] Glarborg,[16] and Konnov.[22] Methane, which is always present in the exhaust of these engines, was found to have a very strong impact on the reactivity of NO_x and NH_3; the onset of conversion of these two components was decreased by nearly 200 K in comparison with a mixture free of methane and NO_2. This mutual promoting effect was traced back to NO and NO_2 first enhancing CH_4 oxidation due to CH_3O

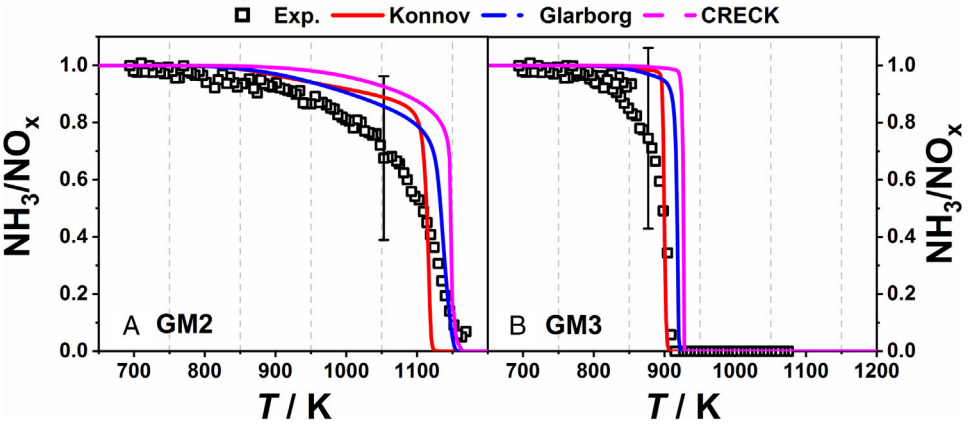

FIGURE 13 NH_3/NO_x ratio from experimental and simulation results for GM2 ($NH_3/NO/NO_2$) and GM3 ($NH_3/NO/NO_2/CH_4$). The experimental uncertainty is indicated at only one temperature point for clarity [Color figure can be viewed at wileyonlinelibrary.com]

radical formation (CH_3 oxidation with NO/NO_2). CH_3O is further oxidized to CH_2O and in the end CO_2 producing important radicals, which further enhance NO and NH_3 reactivity. Therefore, a small amount of CH_4 in the exhaust gas might be considered advantageous regarding the required temperature of $DeNO_x$ processes. The impact of NO_2 is significant as well but not so pronounced. The influences of CO and C_2H_4 added to the mixture on the reactivity remained rather small. Since NH_3 and NO_x are converted to a very different extent, and NO_x is even produced by NH_3 oxidation, the NH_3/NO_x ratio decreases significantly with increasing temperatures. Even for rather moderate temperatures, the function of NH_3 as reducing agent for NO_x in a SCR system is limited by the onset of gas-phase reactions, which has severe implications on the ammonia (urea-water solution) dosing strategy. Obviously, quantitative models are needed to describe the homogeneous conversion of NH_3 and NO_x in the presence of CH_4 in the exhaust of lean-operated natural gas engines.

The three mechanisms used to simulate these effects were able to predict all major trends and the experimentally observed temperature dependence of the NH_3/NO_x ratio qualitatively well for all five mixtures. Since all three mechanisms were not developed using conditions we applied here, we very much appreciate their impressive ability to model the NH_3 and NO_x reactivity under these scarcely investigated conditions. Both model-based designs of the aftertreatment system and optimization of the ammonia dosing strategy request quantitative model predictions. Therefore, we would like to recommend further developments of these mechanisms specifically for these conditions with highly diluted concentrations (on the order of hundreds of ppm) of NH_3, NO_x, and CH_4 at moderate temperatures. Here, we began to analyze the kinetics of these mechanisms for the specific conditions of this application in more detail, which led to different behaviors of the individual mechanisms. The reaction flow analyses reveal differences regarding main C-N interaction. A small underprediction of NO mole fractions was found for the Konnov mechanism, which could be influenced by an underestimation of the importance of the reaction sequence $NH_2 \rightarrow H_2NO \rightarrow HNO \rightarrow NO$. According to the reaction flow analyses, this sequence is apparently more important in both Glarborg and CRECK mechanisms. Regarding the exhaust gas compositions, intense reactions in the gas phase can be expected involving both nitrogen and carbon chemistry. With this analysis, we can give some hints in which direction further mechanism development should be conducted and we would like to encourage further research here.

As we have learnt, homogeneous gas-phase reactions affect the concentrations of NH_3 and NO in the exhaust pipe of lean-operated natural gas engines. They are likely to also occur inside the channels of the catalytic converters, that is, the NH_3-SCR and the oxidation catalysts positioned close to the engine. Hence, we can expect some interference between homogeneous gas-phase reactions and heterogeneous catalytic reactions inside the converter as observed for many other systems such as by the Mantzaras group for catalytically supported combustion.[45] Consequently, we will next study the interaction of gas-phase and surface reactions inside the catalytic converters.

ACKNOWLEDGEMENTS

Support by the Deutsche Forschungsgemeinschaft (KO 1363/34-1 and DE659/12-1) is gratefully acknowledged. Furthermore, we acknowledge Steinbeis GmbH & Co. KG für Technologietransfer (STZ 240 Reaktive Strömung) for a cost-free license of DETCHEM.

Open access funding enabled and organized by Projekt DEAL.

ORCID

Steffen Schmitt https://orcid.org/0000-0002-0076-0961
Lena Ruwe https://orcid.org/0000-0002-6244-1755

REFERENCES

1. Gremminger A, Pihl J, Casapu M, Grunwaldt JD, Toops TJ, Deutschmann O. PGM based catalysts for exhaust-gas aftertreatment under typical diesel, gasoline and gas engine conditions with focus on methane and formaldehyde oxidation. *Appl Catal B Environ*. 2020;265:118571. https://doi.org/10.1016/j.apcatb.2019.118571.
2. Ayala A, Kado NY, Okamoto RA, et al. Regulated Pollutants and Project Overview Linked references are available on JSTOR for this article: Diesel and CNG Heavy-duty Transit Bus Emissions Multiple Driving Schedules : Regulated Pollutants and Overview. 2020, 111.
3. Börnhorst M, Langheck S, Weickenmeier H, Dem C, Suntz R, Deutschmann O. Characterization of solid deposits from urea water solution injected into a hot gas test rig. *Chem Eng J*. 2019;377:119855. https://doi.org/10.1016/j.cej.2018.09.016.
4. Gremminger AT, Pereira de Carvalho HW, Popescu R, Grunwaldt J-D, Deutschmann O. Influence of gas composition on activity and durability of bimetallic Pd-Pt/Al_2O_3 catalysts for total oxidation of methane. *Catal Today*. 2015;258:470-480.
5. Gremminger A, Lott P, Merts M, Casapu M, Grunwaldt J-D, Deutschmann O. Sulfur poisoning and regeneration of bimetallic Pd-Pt methane oxidation catalysts. *Appl Catal B Environ*. 2017;218:833-843.
6. Rammelt T, Torkashvand B, Hauck C, Böhm J, Gläser R, Deutschmann O. Nitric oxide reduction of heavy-duty diesel offgas by NH_3-SCR in front of the turbocharger. *Emiss Control Sci Technol*. 2017;3:275-288.
7. Smith J, Phillips J, Park UV, et al. Homogeneous chemistry in lean-burn exhaust mixtures. *J Phys Chem A*. 1997;5639:9157-9162.
8. Torkashvand B, Lott P, Zengel D, et al. Homogeneous oxidation of light alkanes in the exhaust of turbocharged lean-burn gas engines. *Chem Eng J*. 2019;377:119800. https://doi.org/10.1016/J.CEJ.2018.08.186.
9. Günter T, Pesek J, Schäfer K, et al. Cu-SSZ-13 as pre-turbine NOx-removal-catalyst: impact of pressure and catalyst poisons. *Appl Catal B Environ*. 2016;198:548-557.
10. Rota R, Zanoelo ÉF, Antos D, Morbidelli M, Carra S. Analysis of the thermal DeNOx process at high partial pressure of reactants. *Chem Eng Sci*. 2000;55:1041-1051.
11. Kasuya F, Glarborg P, Johnsson JE, Dam-Johansen K. The thermal DeNO$_x$ process: influence of partial pressures and temperature. *Chem Eng Sci*. 1995;50:1455-1466.
12. Glarborg P, Dam-Johansen K, Miller JA, Kee RJ, Coltrin ME. Modeling the thermal DENO$_x$ process in flow reactors. Surface effects and nitrous oxide formation. *Int J Chem Kinet*. 1994;26:421-436.
13. Song Y, Hashemi H, Christensen JM, Zou C, Marshall P, Glarborg P. Ammonia oxidation at high pressure and intermediate temperatures. *Fuel*. 2016;181:358-365.
14. Locci C, Vervisch L, Farcy B, Domingo P, Perret N. Selective non-catalytic reduction (SNCR) of nitrogen oxide emissions: a perspective from numerical modeling, flow. *Turbul Combust*. 2018;100:301-340.
15. Wargadalam VJ, Löffler G, Winter F, Hofbauer H. Homogeneous formation of NO and N_2O from the oxidation of HCN and NH_3 at 600–1000°C. *Combust Flame*. 2000;120:465-478.
16. Glarborg P, Miller JA, Ruscic B, Klippenstein SJ. Modeling nitrogen chemistry in combustion. *Prog Energy Combust Sci*. 2018;67:31-68.
17. Lyon RK. The NH_3-NO-O_2 reaction. *Int J Chem Kinet*. 1976;8:315-318.
18. Miller JA, Bowman CT. Mechanism and modeling of nitrogen chemistry in combustion. *Prog Energy Combust Sci*. 1989;14:287-338.
19. Bagheri G, Ranzi E, Pelucchi M, Parente A, Frassoldati A, Faravelli T. Comprehensive kinetic study of combustion technologies for low environmental impact: mILD and OXY-fuel combustion of methane. *Combust Flame*. 2020;212:142-155.
20. Ranzi E, Cavallotti C, Cuoci A, Frassoldati A, Pelucchi M, Faravelli T. New reaction classes in the kinetic modeling of low temperature oxidation of n-alkanes. *Combust Flame*. 2015;162:1679-1691.
21. Ranzi E, Frassoldati A, Stagni A, Pelucchi M, Cuoci A, Faravelli T. Reduced kinetic schemes of complex reaction systems: fossil and biomass-derived transportation fuels. *Int J Chem Kinetics*. 2014;46:512-542.
22. Konnov AA. Implementation of the NCN pathway of prompt-NO formation in the detailed reaction mechanism. *Combust Flame*. 2009;156:2093-2105.
23. Hemken C, Burke U, Lam K-Y, et al. Toward a better understanding of 2-butanone oxidation: detailed species measurements and kinetic modeling. *Combust Flame*. 2017;184:195-207.
24. Jin H, Pieper J, Hemken C, Bräuer E, Ruwe L, Kohse-Höinghaus K. Chemical interaction of dual-fuel mixtures in low-temperature oxidation, comparing n-pentane/dimethyl ether and n-pentane/ethanol. *Combust Flame*. 2018;193:36-53.
25. Schenk M, Leon L, Moshammer K, et al. Detailed mass spectrometric and modeling study of isomeric butene flames. *Combust Flame*. 2013;160:487-503.
26. Goodwin DG, Speth RL, Moffat HK, Weber BW, Cantera: An object-oriented software toolkit for chemical kinetics, thermodynamics, and transport processes (2019). https://doi.org/10.5281/zenodo.1174508.
27. Reaction Design: San Diego, CHEMKINPro 15112 (2011).
28. Deutschmann O, Tischer S, Kleditzsch S, et al. DETCHEM Software package, 2.7 ed., Karlsruhe (2018), www.detchem.de.
29. Lyon RK. Thermal DeNO$_x$ controlling nitrogen oxides emissions by a noncatalytic process. *Environ Sci Technol*. 1987;21:231-236.
30. Klippenstein SJ, Harding LB, Glarborg P, Miller JA. The role of NNH in NO formation and control. *Combust Flame*. 2011;158:774-789.
31. Miller JA, Klippenstein SJ. Theoretical considerations in the NH_2 + NO reaction. *J Phys Chem A*. 2000;104:2061-2069.
32. Miller JA, Glarborg P. Modeling the thermal De-NOx process: closing in on a final solution. *Int J Chem Kinet*. 1999;31:757-765.
33. Miller JA, Branch MC, Kee RJ. A chemical kinetic model for the selective reduction of nitric oxide by ammonia. *Combust Flame*. 1981;43:81-98.
34. Stief LJ, Brobst WD, Nava DF, Borkowski RP, Michael JV. Rate constant for the reaction NH_2+NO from 216 to 480 K. *J Chem Soc Faraday Trans 2*. 1982;78:1391.

35. Bae SW, Roh SA, Kim SD. NO removal by reducing agents and additives in the selective non-catalytic reduction (SNCR) process. *Chemosphere*. 2006;65:170-175.
36. Rota R, Antos D, Zanoelo EF, Carra S. Experimental study and kinetic modelling of nitric oxide reduction with ammonia. *Combust Sci Technol*. 2001;163:25-47.
37. Alzueta MU, Røjel H, Kristensen PG, Glarborg P, Dam-Johansen K. Laboratory study of the $CO/NH_3/NO/O_2$ system: implications for hybrid reburn/SNCR strategies. *Energy Fuels*. 1997;11:716-722.
38. Villamaina R, Nova I, Tronconi E, Maunula T, Keenan M. The effect of CH_4 on NH_3-SCR over metal-promoted zeolite catalysts for lean-burn natural gas vehicles. *Top Catal*. 2018;61:1974-1982.
39. Faravelli T, Frassoldati A, Ranzi E. Kinetic modeling of the interactions between NO and hydrocarbons in the oxidation of hydrocarbons at low temperatures. *Combust Flame*. 2003;132:188-207.
40. Bromly JH, Barnes FJ, Muris S, You X, Haynes BS. Kinetic and thermodynamic sensitivity analysis of the NO-sensitised oxidation of methane. *Combust Sci Technol*. 1996;115:259-296.
41. Konnov AA, Ning Zhu J, Bromly JH, Zhang DK. The effect of NO and NO_2 on the partial oxidation of methane: experiments and modeling. *Proc Combust Inst*. 2005;30:1093-1100.
42. Torkashvand B, Lott P, Zengel D, et al. Homogeneous oxidation of light alkanes in the exhaust of turbocharged lean-burn gas engines. *Chem Eng J*. 2019;377:119800. https://doi.org/10.1016/J.CEJ.2018.08.186.
43. Hori M, Matsunaga N, Marinov N, Pitz W, Westbrook C. An experimental and kinetic calculation of the promotion effect of hydrocarbons on the NO-NO_2 conversion in a flow reactor. *Symp Combust*. 1998;27:389-396.
44. Kristensen PG, Glarborg P, Dam-Johansen K. Nitrogen chemistry during burnout in fuel-staged combustion. *Combust Flame*. 1996;107:211-222.
45. Sui R, Mantzaras J, Es-Sebbar ET, Bombach R. Hetero-/homogeneous combustion of fuel-lean CH_4 /O_2 /N_2 mixtures over PdO at elevated pressures. *Proc Combust Inst*. 2019;37:5465-5472.

SUPPORTING INFORMATION

Additional supporting information may be found online in the Supporting Information section at the end of the article.

How to cite this article: Schmitt S, Schwarz S, Ruwe L, et al. Homogeneous conversion of NO_x and NH_3 with CH_4, CO, and C_2H_4 at the diluted conditions of exhaust-gases of lean operated natural gas engines. *Int J Chem Kinet*. 2020;1-17. https://doi.org/10.1002/kin.21435